

The response of the Fe $K\alpha$ line to changes in the X-ray illumination of accretion discs

D. R. Ballantyne^{1*} and R. R. Ross²

¹*Institute of Astronomy, Madingley Road, Cambridge CB3 0HA*

²*Physics Department, College of the Holy Cross, Worcester, MA 01610, USA*

22 October 2018

ABSTRACT

X-ray reflection spectra from photoionized accretion discs in active galaxies are presented for a wide range of illumination conditions. The energy, equivalent width (EW) and flux of the Fe $K\alpha$ line are shown to depend strongly on the ratio of illuminating flux to disc flux, F_x/F_{disc} , the photon index of the irradiating power-law, Γ , and the incidence angle of the radiation, i . When $F_x/F_{\text{disc}} \leq 2$ a neutral Fe $K\alpha$ line is prominent for all but the largest values of Γ . At higher illuminating fluxes a He-like Fe $K\alpha$ line at 6.7 keV dominates the line complex. With a high-energy cutoff of 100 keV, the thermal ionization instability seems to suppress the ionized Fe $K\alpha$ line when $\Gamma \leq 1.6$. The Fe $K\alpha$ line flux correlates with F_x/F_{disc} , but the dependence weakens as iron becomes fully ionized. The EW is roughly constant when F_x/F_{disc} is low and a neutral line dominates, but then declines as the line progresses through higher ionization stages. There is a strong positive correlation between the Fe $K\alpha$ EW and Γ when the line energy is at 6.7 keV, and a slight negative one when it is at 6.4 keV. This is a potential observational diagnostic of the ionization state of the disc. Observations of the broad Fe $K\alpha$ line which take into account any narrow component would be able to test these predictions. Ionized Fe $K\alpha$ lines at 6.7 keV are predicted to be common in a simple magnetic flare geometry. A model which includes multiple ionization gradients on the disc is postulated to reconcile the results with observations.

Key words: accretion, accretion discs – line: profiles – galaxies: active – X-rays: general

1 INTRODUCTION

The discovery of the iron $K\alpha$ line and Compton reflection in the X-ray spectra of accreting black holes was an important step in the understanding of the central engine (Mushotzky, Done & Pounds 1993). These features were predicted to result from the reprocessing of X-rays by an optically thick and cold medium (Lightman & White 1988; Guilbert & Rees 1988; George & Fabian 1991; Matt, Perola & Piro 1991), quite likely the accretion disc itself. This was spectacularly confirmed by the ASCA observation of a broad Fe $K\alpha$ line in the X-ray spectrum of the bright Seyfert 1 galaxy MCG–6-30-15 (Tanaka et al. 1995). The profile of this line was well fit by a model of line emission from relativistically moving material within 10 Schwarzschild radii of a supermassive black hole (Fabian et al. 1989). Alternative explanations for such a broad line suffer from physical inconsistencies and/or fine-tuning of model parameters (Fabian et al. 1995; Reynolds & Wilms 2000). Suddenly a potentially powerful probe of accretion and black hole physics was observationally accessible (Fabian et al. 2000). Many other active galactic nuclei (AGN) were subsequently observed by ASCA in search of a broad Fe $K\alpha$ line, and, although most of the detections

were of far less quality than the one of MCG–6-30-15, the mean line profile of a sample of Seyferts seemed to be broadened in a similar manner (Nandra et al. 1997a; Yaqoob et al. 2002).

Since AGN themselves have quite variable X-ray continua, it was anticipated that the Fe $K\alpha$ line should also change over an observation. The largest dataset has come from long observations of MCG–6-30-15 where the line is seen to sometimes drastically change energy (Iwasawa et al. 1996, 1999), and its flux varies independently of the continuum (Vaughan & Edelson 2001). This last property, also seen in other objects (Wang et al. 1999; Nandra et al. 1999; Chiang et al. 2000; Wang, Wang & Zhou 2001; Weaver, Gelbord & Yaqoob 2001), is contrary to the predictions of the simple reflection scenario, which predicts the line variations should track the continuum. The fact that this is not observed suggests a more complicated and dynamic pattern of illumination on the disc (Reynolds 2000) such as in the model of irradiation by magnetic flares in a patchy corona (Galeev, Rosner & Vaiana 1979; Haardt & Maraschi 1991; Haardt, Maraschi & Ghisellini 1994; Merloni & Fabian 2001). These flares may be rotating (Ruszkowski 2000), outflowing (Beloborodov 1999; Malzac, Beloborodov & Poutanen 2001) and/or temporally connected (Poutanen & Fabian 1999; Merloni & Fabian 2001), and so they will clearly have an impact on the

* drb@ast.cam.ac.uk

observed Fe $K\alpha$ line due to the changing pattern of radiation on the surface of the disc.

Many models of X-ray reflection from AGN-like accretion discs have been published (e.g. Ross & Fabian 1993; Życki et al. 1994; Magdziarz & Zdziarski 1995; Ross, Fabian & Young 1999), but they have not progressed to the same dynamic level as the models of accretion disc coronae. The best current models compute the reflection spectrum from a photoionized layer on the surface of an accretion disc in hydrostatic equilibrium (Nayakshin, Kazanas & Kallman 2000; Ballantyne, Ross & Fabian 2001; Róžańska et al. 2001). If discs are anything like what standard theory predicts, then these calculations should be able to make specific predictions about reflection spectra (e.g. Nayakshin 2000; Nayakshin & Kallman 2001).

Here, we compute such spectra from an AGN accretion disc over a wide range of illumination conditions, and examine the behaviour of the energy, equivalent width (EW) and flux of the Fe $K\alpha$ line. Our approach differs from that of Nayakshin & Kallman (2001) or Życki & Róžańska (2001) by concentrating on the observationally accessible changes to the Fe $K\alpha$ line. The parameters are chosen so that conditions appropriate for both flaring and quiescent regions of the disc are explored. Comparison of the model predictions with time-averaged data (to avoid any non-equilibrium effects) may allow constraints to be placed on how discs are irradiated.

The paper is structured as follows. Section 2 describes the model, the assumptions, and the range of parameters that are treated. The results of the calculations and a discussion of the evolution of the Fe $K\alpha$ line profile, flux and EW are given in Section 3. A discussion of the results is given in Section 4 before Section 5 summarizes the primary conclusions.

2 COMPUTATIONS

We employ the code of Ross & Fabian (1993), recently extended by Ballantyne et al. (2001), to calculate the X-ray reflection spectrum from the ionized layer on the surface of an AGN accretion disc. The details of the calculations are described in the above two papers (see also Ross (1978) and Ross, Weaver & McCray 1978), and so only a brief description is given here.

The model calculates the thermal, ionization and density structure of the top five¹ Thomson depths of an accretion disc that is irradiated by an external source of X-rays from above, and a soft blackbody from the disc below. The calculation is one-dimensional, with the height of the bottom of the atmosphere given by the disc equations of Merloni, Fabian & Ross (2000) in the gas-pressure dominated regime and assuming $\alpha = 0.1$. The flux of soft radiation entering the layer from below is assumed to result from viscous heating deep in the disc and is calculated using the standard equation from Shakura & Sunyaev (1973). The impinging hard X-rays are in the form of a power-law with photon index Γ (so that photon flux $\propto E^{-\Gamma}$), which strikes the surface with net flux F_x and at an angle of i degrees to the normal. The incident X-rays extend from 1 eV and terminate with a sharp cutoff at 100 keV.

The incident radiation is transferred analytically using a one-stream approximation (e.g., Rybicki & Lightman 1979). Diffuse radiation within the layer (i.e., incident X-rays that have undergone

Compton scattering, other emission from the gas itself, and the soft photons working their way outward from the disc below) is treated via the Fokker-Planck/diffusion approximation (Ross et al. 1978), while the Fe $K\alpha$ line is treated in detail via escape and destruction probabilities assuming a Lorentz line profile (see Ross 1978, Ross & Fabian 1993). Hydrogen and helium are assumed to be fully ionized everywhere within the layer, and the following ionization stages of the most abundant metals are treated: C V–VII, O V–IX, Mg IX–XIII, Si XI–XV, and Fe XVI–XXVII. The elemental abundances are given by Morrison & McCammon (1983).

The major differences between this code and the one presented by Nayakshin et al. (2000) are in the method of radiative transfer (we use Fokker-Planck/diffusion, as opposed to a variable Eddington factor scheme) and in the level of detail that atomic physics is treated (Nayakshin et al. (2000) employ XSTAR for the photoionization calculations and so includes many more transitions than our code). However, comparisons between the two programs yield only minor qualitative differences in the output spectra, particularly around the Fe $K\alpha$ line (Péquignot et al. 2002).

To isolate the Fe $K\alpha$ variations due to a changing illumination pattern, the accretion disc parameters were set to representative values. A typical black hole mass of $10^8 M_\odot$ (Gebhardt et al. 2000) was used in the calculations, as was an accretion rate of 0.001 of the Eddington rate, which seems typical of some X-ray bright Seyfert 1 galaxies (Morales & Fabian 2002). A radius of 7 Schwarzschild radii was selected for where the reflection takes place, but we do not take into account relativistic blurring. With these parameters, the soft flux entering the atmosphere from below is $F_{\text{disc}} = 1.2 \times 10^{13} \text{ erg cm}^{-2} \text{ s}^{-1}$, and it is assumed that there is no energy dissipation in the corona. Other choices for these system parameters would result in different Fe $K\alpha$ EWs and fluxes, but the resulting trends with the illumination parameters should not be affected (Sect. 3.3).

Models were calculated for $1.5 \leq \Gamma \leq 2.1$, which is the range most often observed for Seyfert 1 galaxies (Nandra et al. 1997a), and with the incident flux covering $F_x/F_{\text{disc}} \approx 0.5 - 270$. To test for geometrical effects (which may be important for magnetic flares where the size of the hard X-ray emitting region is much smaller than the disc), for each value of Γ and F_x models were calculated for X-ray incidence angles $20 \leq i \leq 80$ degrees in steps of 20 degrees. Finally, we neglect the effects of inclination along the line of sight, but since this does not depend on the disc or illumination model, earlier results (e.g., Matt, Fabian & Ross 1996) will still apply.

3 RESULTS

3.1 Fe $K\alpha$ line profiles

The properties of the Fe $K\alpha$ line depend greatly on the ionization state of the gas (e.g., Matt, Fabian & Ross 1993, 1996; Ross et al. 1999). When the gas is only weakly ionized or neutral (so that Fe I–XVI are the dominant ionization states), a strong line appears at 6.4 keV and the associated absorption edge is close to 7.1 keV. As the gas becomes more ionized, intermediate Fe states such as Fe XVII–XXIII are dominant. However, the $K\alpha$ lines from these ions are preferentially suppressed due to Auger destruction (Ross, Fabian & Brandt 1996). It is not until the gas becomes so ionized that He-like iron (Fe XXV) is the dominant species that the observed $K\alpha$ line shifts in energy. This ion has a large fluorescent yield resulting in a strong line and absorption edge at 6.7 keV and

¹ When $F_x/F_{\text{disc}} = 270$ a total Thomson depth of 10 was used to extend the computational domain beyond the layer that is highly ionized by the illuminating radiation.

~ 8.5 keV, respectively². The line from hydrogenic Fe at 6.97 keV is also present in these situations, but is weaker than the helium-like line because of resonant scattering. Finally, it is possible for Fe to be fully stripped and neither a line nor an edge will be imprinted on the reflection spectrum.

In variable density models it is not possible to describe the spectrum by assigning an ionization parameter to it. However, the general evolution of the Fe K α line that was described above is seen in these new calculations, but the addition of a realistic density structure can create significant departures from this trend. Figure 1 shows how the Fe K α region of the reflection spectrum can vary for two different values of F_x/F_{disc} when the photon index of the illuminating spectrum changes. At the lower value of F_x/F_{disc} , the Fe K α emission lines become more ionized (i.e., has a significant He-like component) with larger values of Γ than with smaller values. This is possibly counter-intuitive because the harder irradiating spectra have more Fe-ionizing power than the softer ones. However, when F_x/F_{disc} is increased (the bottom panel of Fig. 1) the situation is reversed, and the Fe K α line becomes highly ionized and weak at the lowest values of Γ .

The explanation for this behaviour is illustrated in Figure 2. The plots show that when $\Gamma = 1.5$ the temperature of the photoionized gas falls abruptly from a very hot (\sim Compton temperature) fully ionized phase to a cold, recombined phase. Nayakshin et al. (2000) showed that such behaviour is due to the well-known thermal ionization instability of gases in pressure balance (e.g., Krolik, McKee & Tarter 1981). There is a negligible fraction of gas with intermediate ionization states, so, when F_x/F_{disc} is relatively small, only a neutral Fe K α line is emitted with any real strength³. At higher values of F_x/F_{disc} the incident radiation ionizes further into the atmosphere and the transition occurs at a non-negligible Thomson depth. Few K-shell ionizing photons can traverse this layer to the neutral material below without being scattered outwards or absorbed by a higher ionized species of iron. Therefore, at higher values of F_x/F_{disc} , the line weakens and disappears at the lowest values of Γ . As the photon-index is increased, the maximum temperature of the gas decreases (Guilbert, Fabian & McCray 1983 and Sect. 4.1) and the instability cannot operate. Other ionized species of Fe can exist near the surface and a He-like line appears in the spectrum. From Fig. 1 we see that one effect of this instability is to suppress ionized Fe K α lines when $\Gamma \leq 1.6$ (but see Sect. 4.1).

A typical example of how the Fe K α line evolves with increasing F_x/F_{disc} is shown in Figure 3. When $F_x/F_{\text{disc}}=0.5$ or 1.0 then the surface of the accretion disc is not highly ionized and a neutral line at 6.4 keV dominates the line profile. As F_x/F_{disc} is increased the He-like line strengthens and then weakens as the atmosphere is further ionized. Also, the line profile gradually broadens due to Compton scattering. This trend is similar to the predictions of constant density reflection models (Ross et al. 1999).

Finally, we will briefly discuss the impact of the incidence angle of the incoming radiation. When the angle of the beam is increased, the radiation encounters any specific line-of-sight Thomson depth at a smaller physical depth into the atmosphere. Therefore, the energy is dumped into a smaller physical region, which in-

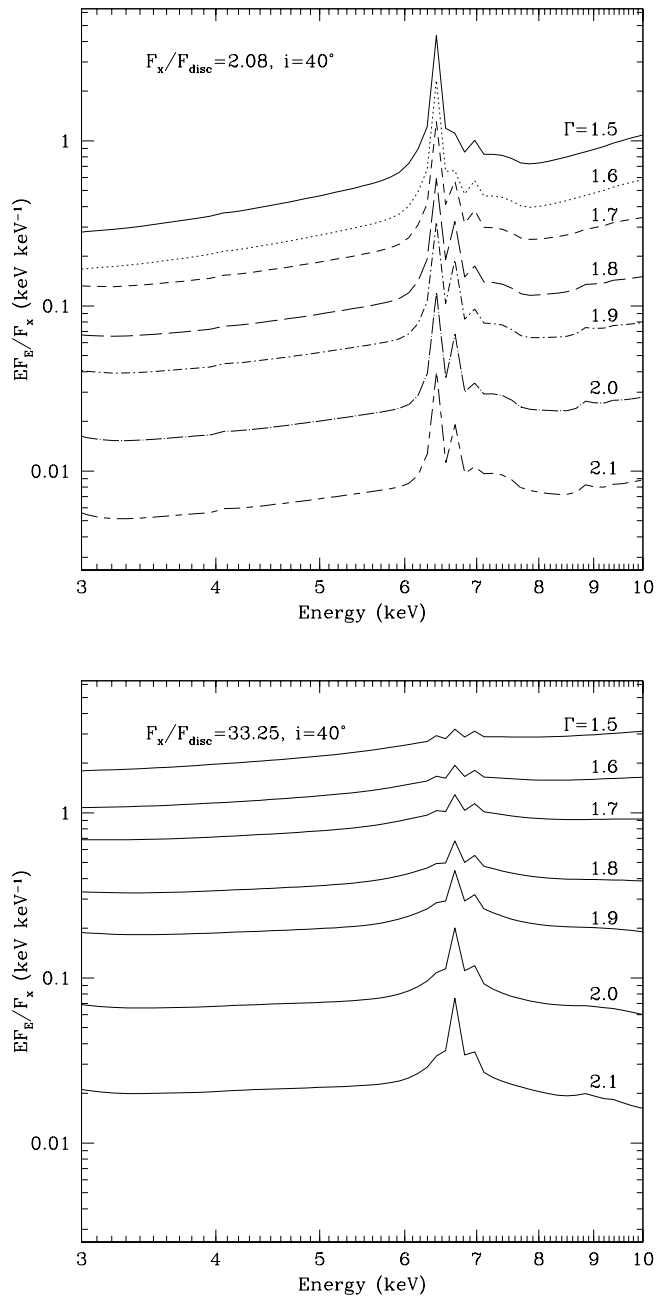


Figure 1. *Top:* The variation in the Fe K α line profile due to changes in the photon index of the illuminating radiation. Γ increases from 1.5 at the top of the plot to 2.1 at the bottom, and the spectra have been vertically offset for clarity. *Bottom:* The same plot as in the other panel, but at a higher value of F_x/F_{disc} . Here, the Fe K α line becomes more ionized at lower Γ , which is opposite to the previous case.

² Oelgoetz & Pradhan (2001) showed that under certain conditions the dielectronic satellite lines of Fe XXV could move the energy centroid of the line closer to 6.6 keV.

³ Thermal conduction between the two temperature zones may be important under some conditions, allowing enough gas at intermediate temperatures to imprint spectral features on the reflection spectrum (Rózańska 1999; Li, Gu & Kahn 2001).

creases the temperature of the gas (see also Nayakshin et al. 2000). When F_x/F_{disc} is relatively small this can enhance the thermal instability, as is shown in the top panel of Figure 4. In that case, the He-like component in the line profile disappears when $i = 80$ degrees. However, when F_x/F_{disc} is greater (the bottom panel of Fig. 4) the line photons are emitted at a significant Thomson depth, and the hot outer layers result in a weaker overall line profile.

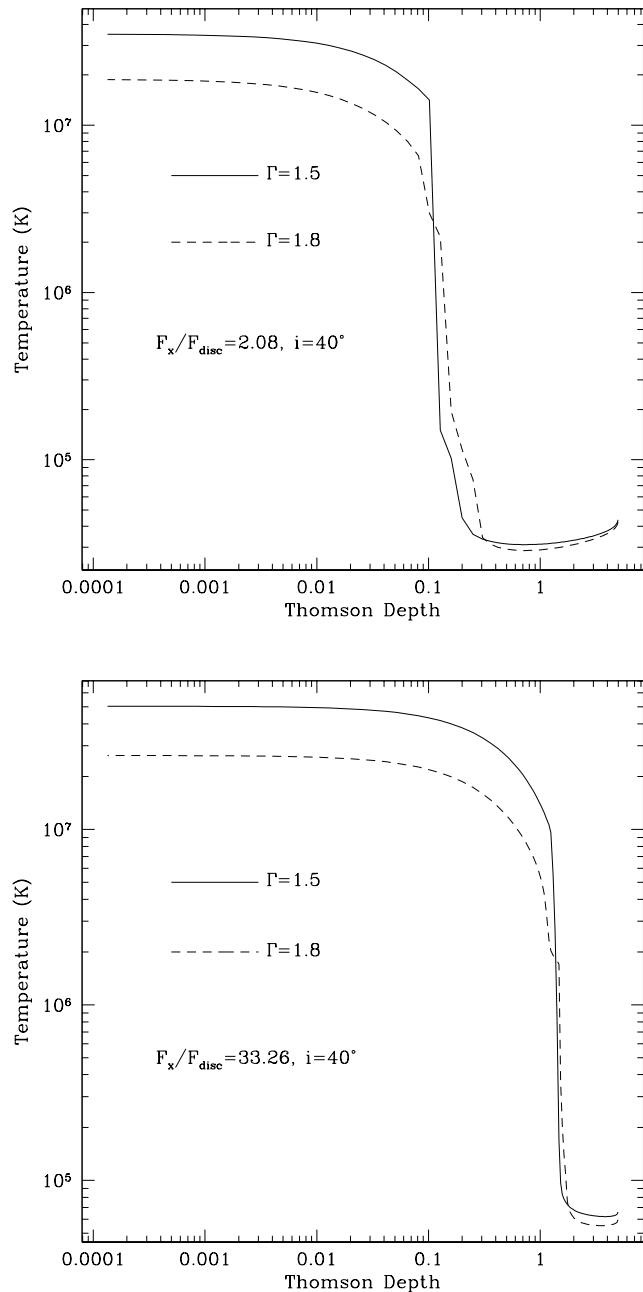


Figure 2. Temperature vs. Thomson Depth plots for the $\Gamma = 1.5$ and 1.8 models that were shown in Fig. 1. When $\Gamma = 1.5$ the temperature falls almost non-continuously from a hot, ionized phase to a cold, recombined phase which is attributed to the thermal ionization instability. As F_x/F_{disc} is increased, the transition occurs at a non-negligible Thomson depth, and less ionizing photons can reach neutral gas without scattering. The $\Gamma = 1.8$ illuminating spectrum cannot heat the gas to as high a temperature, and so the instability does not occur.

3.2 Equivalent width and line flux

The two most important observational diagnostics of the strength of the Fe $K\alpha$ line are its equivalent width (EW) and the flux in the line. Therefore, it is important to investigate how they vary as the illumination of the disc is changed. To facilitate comparison with observations, the illuminating power-law was added to the re-

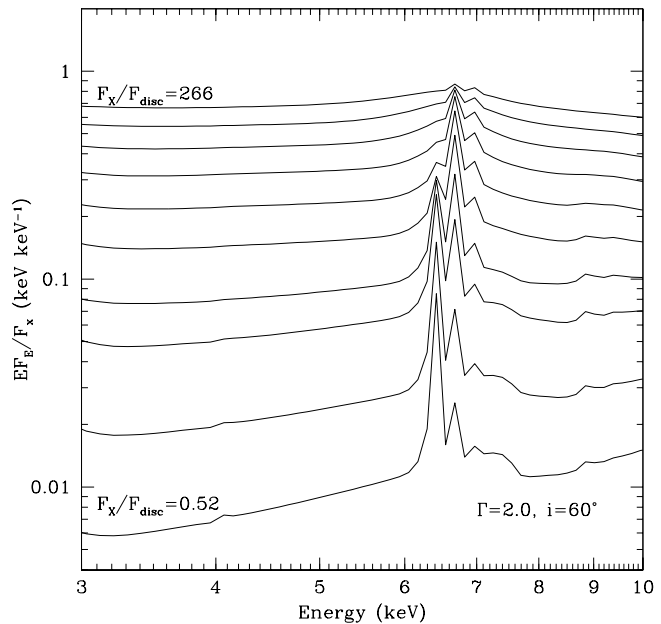


Figure 3. The evolution of the Fe $K\alpha$ line with F_x/F_{disc} for $\Gamma = 2.0$ and an incidence angle of 60 degrees. $F_x/F_{\text{disc}} = 0.52$ for the lower spectrum and increases by factors of two to 270 for the upper spectrum. The spectra have been offset vertically for clarity. The energy evolution of the line is reminiscent of the one predicted by the constant density reflection models.

flection spectrum before the measurements were made. This can be thought of as a reflection fraction of unity, where the reflection fraction measures the strength of the reflected component in an observed spectrum. In the disc-corona model of an AGN, reflection fractions close to one are expected.

The EWs of the Fe $K\alpha$ lines were calculated by performing the following integral on the total reflected+incident spectrum:

$$\text{EW} = \int_{5.50 \text{ keV}}^{7.11 \text{ keV}} \frac{EF_s(E) - EF_c(E)}{EF_c(E)} dE, \quad (1)$$

where $EF_s(E)$ is the spectral flux of the sum, and $EF_c(E)$ is the estimated spectral flux of the continuum at energy E . The continuum was estimated by fitting a straight line to the reflection spectrum between 5.50 and 7.11 keV (see Figure 5). The line flux was computed by an analogous integral over the same limits.

The lower limit of the integration was chosen to take into account any Compton broadening of the line profile, and the upper limit was set to the energy of the photoelectric absorption edge of neutral Fe. Using the models where $F_x/F_{\text{disc}} = 33$, $i = 20$ degrees and $\Gamma = 1.5$ – 2.1 a comparison was made between the EWs calculated by this method and the ones calculated by XSPEC using a simple power-law plus Gaussian model. An ASCA SIS-0 response matrix was used to fake a 500 ks observation for each model spectrum, and the fits were performed on the simulated 3–10 keV data with the width of the Gaussian (σ) fixed at 0.25 keV. The EWs calculated by XSPEC (43–264 eV) were only $\sim 50\%$ larger than those obtained from the above method (26–156 eV). Larger EWs would result if the reflection fraction was greater than unity.

Figure 6 shows how the flux in the Fe $K\alpha$ line depends on the parameters of the illuminating radiation. Each panel plots the line flux (normalized to F_{disc}) versus F_x/F_{disc} for the four different incident angles at a specific photon index. We find that the

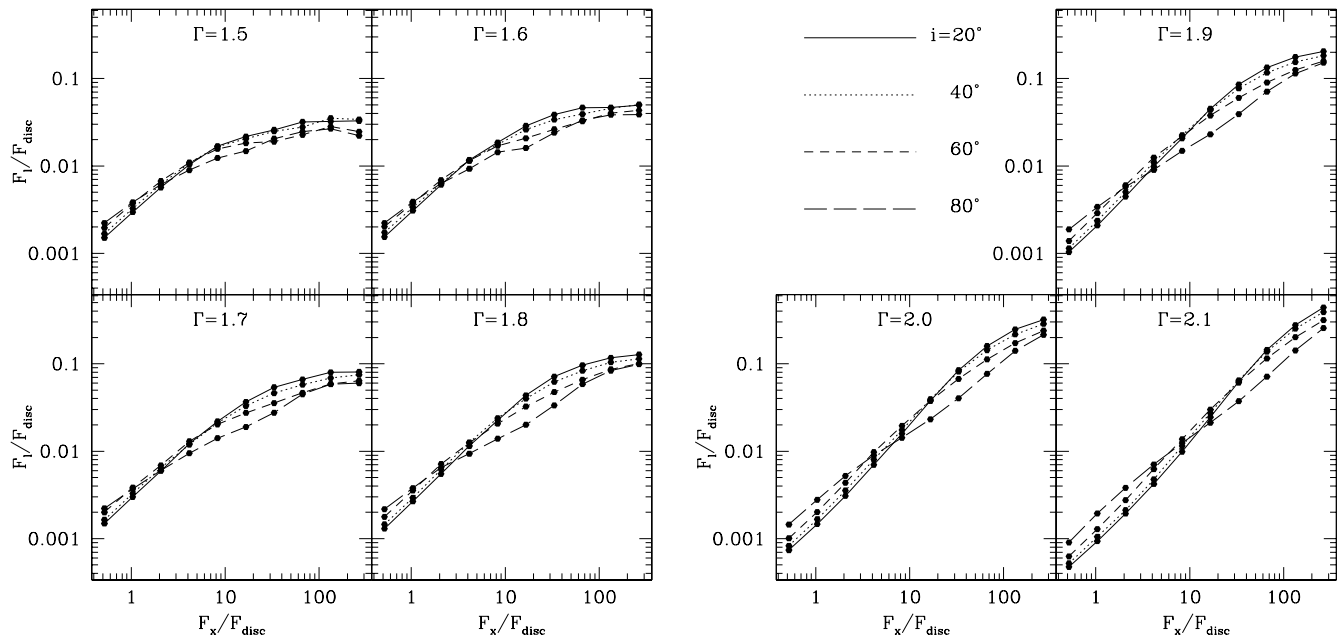


Figure 6. Plots of the Fe K α line flux (normalized to F_{disc}) versus F_x/F_{disc} . The separate panels differentiate between the value assumed for the photon index, Γ , of the incident power-law spectrum. As indicated, the lines in each panel distinguish between different values of the radiation incidence angle. In all cases the line flux correlates with the illuminating flux, but the dependence is much weaker when the line is highly ionized.

line flux is directly proportional to the flux incident on the disc since the amount of energy emitted by the atmosphere must follow the amount that it absorbs. However, the correlation flattens as the line becomes highly ionized and very weak. This is noticeable for $\Gamma \leq 1.7$. An interesting feature about this plot is that it illustrates roughly at which F_x/F_{disc} optical depth effects become important. At low F_x/F_{disc} the line flux increases with increasing incidence angle because line photons are produced closer to the surface and can easily escape (George & Fabian 1991). But this trend reverses at higher values of F_x/F_{disc} where there is a thicker ionized skin and ionizing photons are easily scattered out of the layer before reaching any neutral material. The amount of photons “lost” to scattering increases with i and so the line flux drops as the incidence angle increases. The value of F_x/F_{disc} at which the crossover occurs increases with Γ because greater fluxes are needed to produce a deep enough ionized layer for the softer incident spectra.

Turning to the measurements of the equivalent width, Figure 7 plots the Fe K α EW versus F_x/F_{disc} . At low F_x/F_{disc} a strong neutral Fe K α line is present in all the reflection spectra, so the EWs are high. As F_x/F_{disc} is increased the atmosphere becomes ionized, and where the ionization instability operates ($\Gamma = 1.5$ & 1.6) no other line replaces the neutral line so the EW rapidly becomes very small. For softer illuminating spectra, a He-like line will replace the neutral line, and the EW can remain high, but, as F_x/F_{disc} grows, this line will ultimately weaken and the EW will decrease. As seen in Fig. 6 the incidence angle crossover marks the onset of an optically thick ionized layer at the surface of the atmosphere. This point moves to higher F_x/F_{disc} with larger Γ . Finally, it is worth emphasizing that for $\Gamma \geq 1.8$ the Fe K α EW can stay roughly constant over a factor of about 10 in F_x/F_{disc} .

One other interesting correlation that can be shown with this dataset is illustrated in Figure 8. In this plot the models with $F_x/F_{\text{disc}} \leq 2.08$ are shown with thin solid lines and crosses. In

these cases the Fe K α line complex is dominated by the neutral line for most values of Γ , and there is only a weak dependence of the EW on the photon index. However, when there is a strong ionized component to the line (the curves with solid points), there is a significant positive correlation between the Fe K α EW and Γ . This is a possible explanation for the tentative EW- Γ correlation in the sample of Lubiński & Zdziarski (2001). Furthermore, it may be possible to use these variations as an independent observational diagnostic to determine the ionization state of the accretion disc when other effects (e.g., relativistic broadening) makes it difficult to estimate the energy centroid of the line.

3.3 On the self-consistency of the results

These computations make the zeroth-order assumption that the changes in the irradiating flux, F_x , will not affect the accretion disc structure. In reality, changes in F_x are a result of the changes in disc structure, which will also likely affect F_{disc} . Here, we consider the impact of our assumption on the evolution of the Fe K α line.

An increase in F_x would most probably result from an increase in f , the fraction of the viscous energy dissipated in the corona. However, f is very likely to be a function of the accretion rate \dot{m} . The strength of the dependence of these three parameters on each other is subject to the unknown details of how energy is dissipated and transported in accretion discs, but the dependence of the disc structure on \dot{m} and f is well known (e.g., Svensson & Zdziarski 1994; Merloni et al. 2000). For the low accretion rate assumed for these calculations, the disc is gas-pressure dominated and the scale height of the disc $H \propto \dot{m}^{1/5}(1-f)^{1/10}$. A drop in H will increase the density of the disc, making it more difficult to produce ionized lines. However, this will only occur if F_x is strongly dependent on \dot{m} and/or f . It is likely that as F_x is made larger by an increase in \dot{m} the disc moves from a gas-pressure dom-

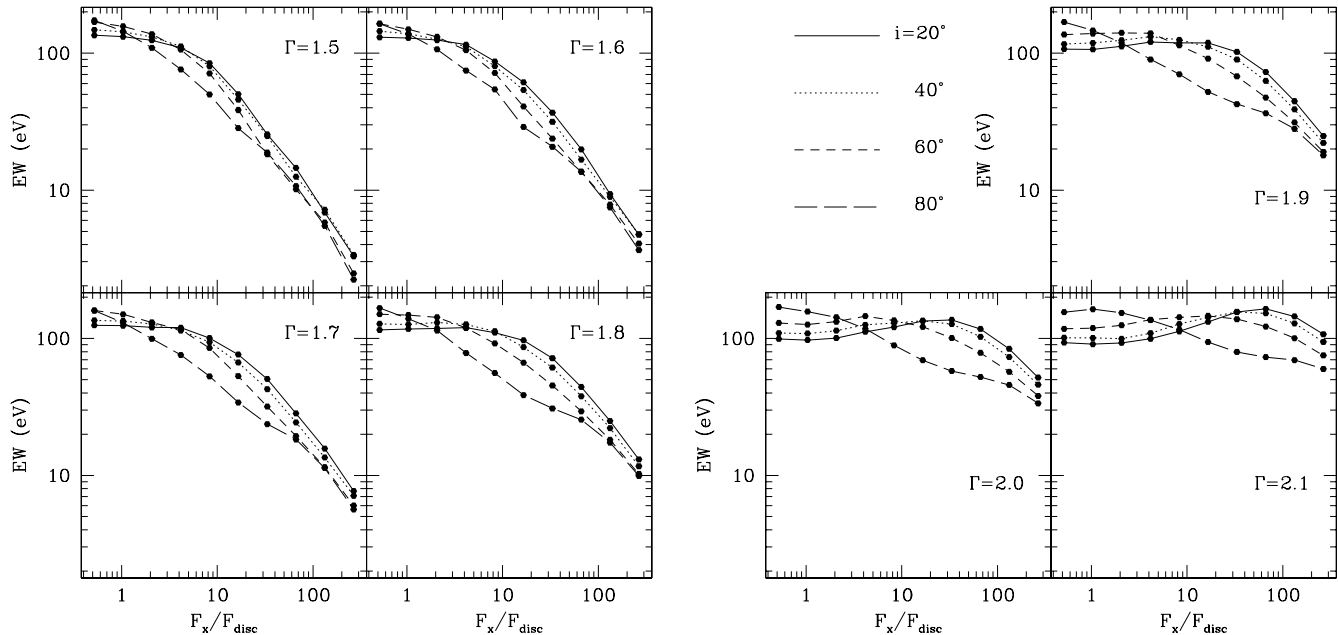


Figure 7. Plots of the Fe K α line equivalent width (EW) versus F_x/F_{disc} . The separate panels differentiate between the value assumed for the photon index, Γ , of the illuminating power-law spectrum. As indicated, the lines in each panel distinguish between different values of the radiation incidence angle. For hard irradiating spectra, the EW will quickly decrease to very small values as the line is ionized and weakened. The decrease is postponed for softer continua where a strong He-like line in the reflection spectrum will keep the EW high.

inated phase to a radiation pressure dominated one. In this case $H \propto \dot{m}(1-f)$, but is much larger in amplitude (by a factor of $\sim 10^3$) than in the gas-pressure dominated regime. Therefore, the density is much lower and ionized Fe K α lines are easily produced over a wide range of F_x/F_{disc} (e.g., $F_x/F_{\text{disc}}=0.48\text{--}2.88$, Ballantyne, Ross & Fabian 2002).

The disc flux $F_{\text{disc}} \propto \dot{m}(1-f)$, and we have seen that ionized lines are common when $F_x/F_{\text{disc}} \gtrsim 2$. Therefore, if F_x has an equal or greater dependence on $\dot{m}(1-f)$ then ionized lines should remain common. However, as commented above, there are very few constraints on the relations between F_x , \dot{m} , and f . Detailed models of energy transport and dissipation in a disc-corona system are required to fully test the validity of these calculations.

4 DISCUSSION

4.1 The role of the Compton temperature

The results presented in the previous section have shown that the thermal ionization instability can influence the evolution of the Fe K α line in certain circumstances. This instability has been investigated previously in the context of broad-line region clouds (Krolik et al. 1981) and irradiated accretion discs (Róžańska 1999; Nayakshin et al. 2000). Here, we combine the previous work with the insight gained by our large dataset to determine, with the minimum of assumptions, the relative importance of the instability on the Fe K α line.

As discussed by Krolik et al. (1981) and Guilbert et al. (1983), the ionization instability is triggered only when the gas temperature is very high (as seen in Figs. 1 & 2). In a photoionized gas in

thermal equilibrium the maximum temperature obtainable⁴ is the Compton temperature T_C :

$$4kT_C \int_{E_l}^{E_h} u_E dE = \int_{E_l}^{E_h} u_E E dE, \quad (2)$$

where u_E is the spectral energy density of the incident radiation field which extends from E_l to E_h . However, this equation overestimates T_C when $E_h \gtrsim 30$ keV because it does not include the Klein-Nishina reduction in Compton heating at higher energies. For radiation in the form of a single power-law $u_E \propto E^{1-\Gamma}$, making the first order Klein-Nishina correction (e.g., Ross et al. 1999) results in

$$kT_C = \frac{(2-\Gamma)E_l}{4(\varepsilon^{2-\Gamma}-1)} \left[\frac{\varepsilon^{3-\Gamma}}{(3-\Gamma)} - \frac{21E_l\varepsilon^{4-\Gamma}}{5m_e c^2(4-\Gamma)} \right], \quad (3)$$

where $\varepsilon \equiv E_h/E_l$ and $\Gamma \lesssim 2.5$. This equation can safely determine T_C for $E_h < 100$ keV.

The dominant factors in determining T_C are $\varepsilon^{3-\Gamma}$ and $\varepsilon^{4-\Gamma}$, thus a larger value of Γ results in a lower Compton temperature. Alternatively, T_C rises if the irradiating spectrum is cut off at larger values of E_l due to the reduction in inverse Compton cooling. For example, with $E_h = 100$ keV and $\Gamma = 2$, $kT_C = 1.3, 1.6$ & 2.1 keV at $E_l = 1, 10$ & 100 eV. This result and Fig. 2 implies that the lower-limit to the X-ray power-law would have to cut off in the hard X-rays, contrary to observations, in order to increase the temperature to high enough values to initiate the instability when $\Gamma = 2$.

Other effects not described by Eq. 3 can also change T_C . As

⁴ In reality, the maximum temperature is less than this limit due to cooling by bremsstrahlung radiation.

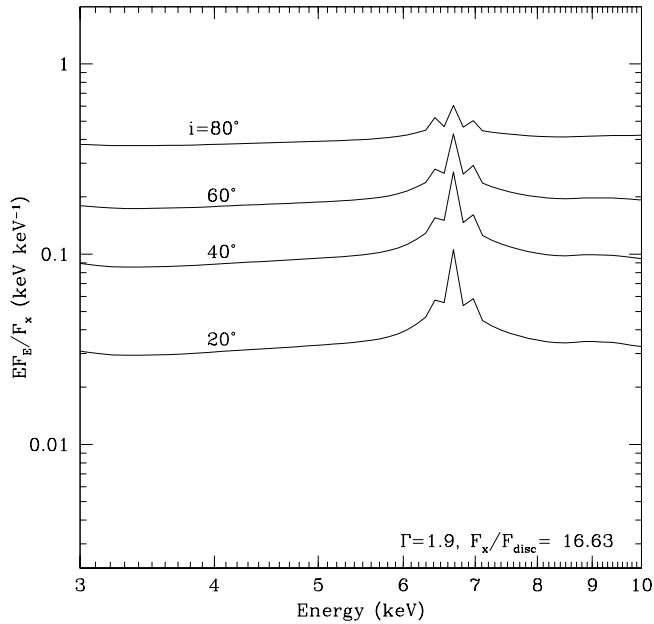
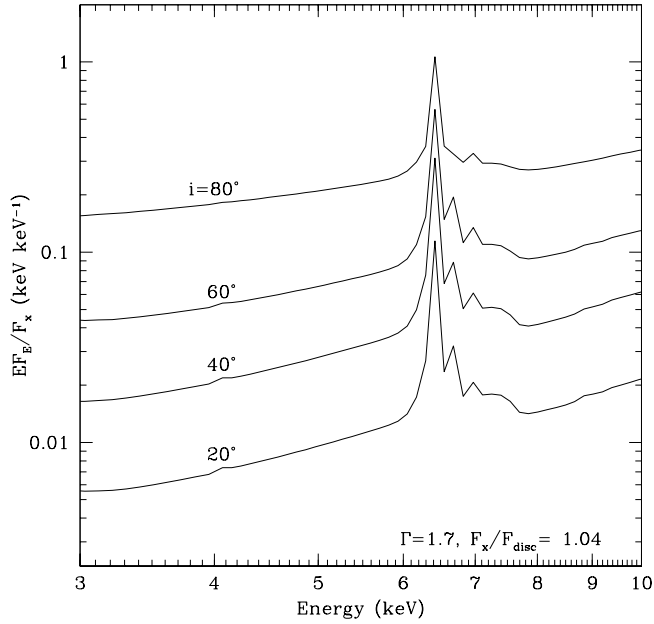


Figure 4. *Top:* The variation in the Fe K α line profile due to changes in the incidence angle of the illuminating radiation. i increases from 20 degrees at the bottom of the plot to 80 degrees at the top, and the spectra have been vertically offset for clarity. *Bottom:* The same plot as in the other panel, but at higher values of F_x/F_{disc} and Γ . The incidence angle has the strongest effect when F_x/F_{disc} is low, as the temperature of the gas increases with i .

already noted in Sect. 3.1, T_C rises with an increase in the incidence angle (Nayakshin et al. 2000), although this can only suppress ionized Fe lines when $\Gamma \sim 2$ if $F_x/F_{\text{disc}} \ll 1$ where they are unlikely to occur for most conditions. Also, T_C can decrease if the disc flux increases due to, say, an increase in accretion rate (Nayakshin & Kallman 2001). The rise in disc flux increases the amount

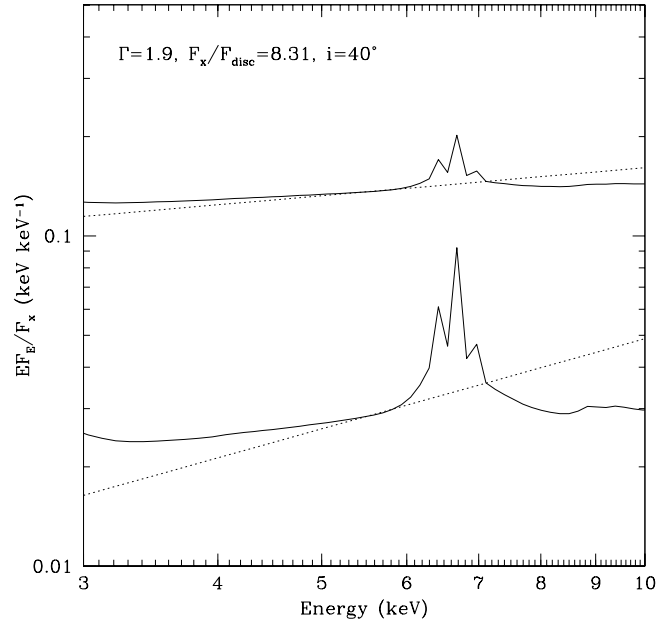


Figure 5. An example of the EW and line flux calculation. The lower spectrum shows a typical computed reflection spectrum, while the upper one has had the illuminating power-law added to it. The continuum was estimated fitting a straight line between 5.5 and 7.1 keV (dotted lines).

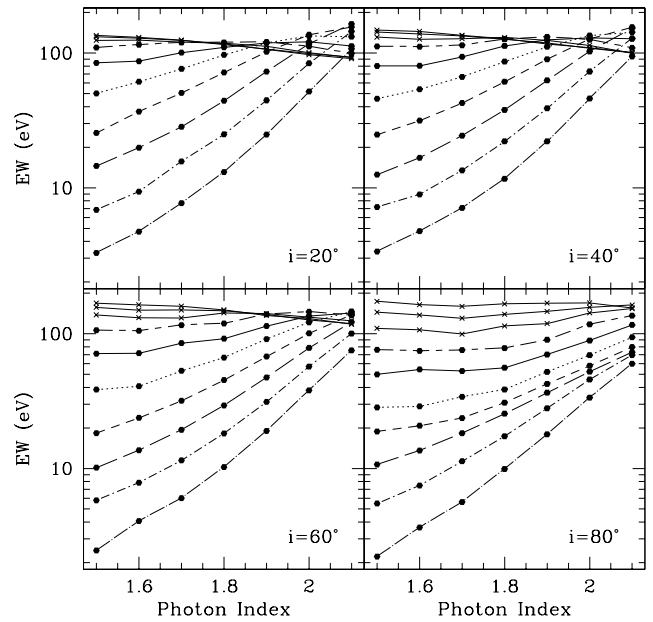


Figure 8. The EW of the Fe K α complex plotted against the photon index of the illuminating power-law. The thin solid lines with the crosses denote models with $F_x/F_{\text{disc}} \leq 2.08$, while the other lines with the solid points (starting with the upper short-dash-long-dash line) trace out the remaining models with F_x/F_{disc} increasing downwards. When there is a significant ionized component to the line the correlation is opposite to the one if the line is predominantly neutral.

of Compton cooling and is, in a sense, equivalent to steepening the incident spectrum.

Observations of a small sample of Seyfert 1 galaxies by *Bep-poSAX* have detected high-energy cutoffs in the power-law continuum between 70 and 300 keV (Matt 2000). Increasing the cutoff energy of the incident power-law will increase the Compton temperature at any value of Γ (possibly to the point of initiating the ionization instability; Nayakshin & Kazanas 2002), but it is difficult to estimate the value of T_C for $E_h > 100$ keV as higher-order Klein-Nishina corrections need to be included. We are therefore placed in the interesting position where the strength of an object at 200 keV can affect its spectral features at 6–7 keV. Models of thermal Comptonization show that the cutoff energy ($\approx 2kT_e$ of the corona) decreases with larger Γ , but the exact form of the relationship depends on the geometry (e.g., Svensson 1996). If AGN with $\Gamma=1.8$ –2.1 are found to have spectral cutoffs < 200 keV then it is likely that these objects will exhibit ionized Fe K α lines. However, it is clear that the calculations need to be extended to higher energies to make more general predictions, and we intend to do this in future work. It is also necessary to obtain more measurements of the overall spectral shape of Seyfert 1 galaxies.

4.2 Comparison with observations

In principle, it is possible to compare the observed long time-scale variations of the broad Fe K α line in AGN with the model predictions. There have been many recent studies on Fe K α variability based on *ASCA* or *RXTE* data (see references listed in Sect. 1 or, for a recent review, Reynolds 2001). However, recent *XMM-Newton* and *Chandra* results have shown that many AGN have narrow Fe K α components in their spectra (Kaspi et al. 2001; Yaqoob et al. 2001; Reeves et al. 2001; Pounds et al. 2001). These lines are expected in AGN unification scenarios where reflection of X-rays may occur from the inner edge of a molecular torus (e.g., Krolik, Madau & Życki 1994). It thus seems likely that narrow Fe K α lines may be common in Seyfert galaxies. These components would have been unresolvable in *ASCA*, and so the published variations in any broad line would be contaminated by this feature.

Nevertheless, it may be possible to compare our predictions to the observations of MCG–6–30–15. Iwasawa et al. (1999) reported that the broad Fe K α line profile of this Seyfert 1 galaxy shifted dramatically to the red during a flare event. There was no noticeable narrow component ($EW < 60$ eV) remaining at 6.4 keV, suggesting that MCG–6–30–15 may harbour only a very weak narrow component. A subsequent long (~ 400 ks) observation of MCG–6–30–15 by *RXTE* reported by Lee et al. (2000) has resulted in a comprehensive study of the Fe K α variability. Lee et al. (2000) split their data into 4 different continuum flux levels and found that the EW of the Fe K α line (as fitted by a Gaussian model) dropped as the flux increased, but that the line flux remained the same. However, if more complex continuum models that included reflection were used, the line flux decreases with increasing continuum flux. A re-analysis of this *RXTE* data by Vaughan & Edelson (2001) found that the line flux varied with time, but it was not correlated with the continuum. As with Lee et al. (2000), Vaughan & Edelson (2001) found that the photon index was correlated with the 2–10 keV flux. Finally, Reynolds (2000) used sophisticated numerical techniques on the *RXTE* data to search for a correlation between the Fe K α line and the continuum over a wider range of timescales than covered by Lee et al. (2000). The search was unsuccessful which suggests that the line flux is uncorrelated with the continuum down to timescales of 0.5 ks.

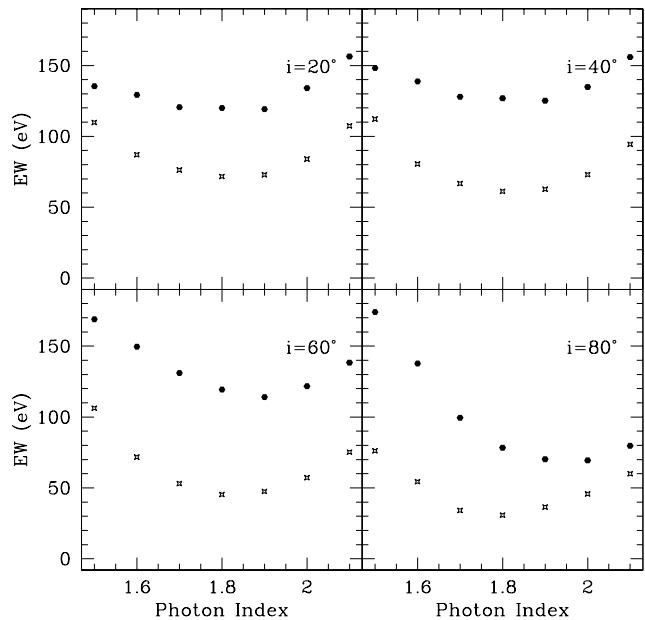


Figure 9. The Fe K α EW plotted against the photon index of the illuminating irradiation, but with F_x/F_{disc} increasing as Γ increases. The solid points denote the evolution when $F_x/F_{\text{disc}} = 0.52$ at $\Gamma = 1.5$, while the stars show the changes when $F_x/F_{\text{disc}} = 4.16$ at $\Gamma = 1.5$. In both cases, F_x/F_{disc} doubles each time Γ increases by 0.1.

Figure 6 predicts that the Fe K α line flux should correlate with the flux striking the disc. Clearly, this does not agree with the observations. The EW was observed to drop with the continuum flux, which does agree with the predictions of Fig. 7. However, the continuum flux in MCG–6–30–15 is observed to correlate with the photon index, which has the opposite effect on the EW (Fig. 8). To give an idea of which effect might dominate the evolution of the Fe K α EW, we plot in Figure 9 how the EW varies with Γ , but tying F_x/F_{disc} to the photon-index. The solid points shows the EW variations when $F_x/F_{\text{disc}} = 0.52$ at $\Gamma = 1.5$, but with F_x/F_{disc} doubling for an increase in Γ of 0.1. In this case the line is mainly neutral and the EW initially drops due to the increase in Γ (recall that increasing F_x/F_{disc} does not change the EW by much when the line is dominated by a 6.4 keV line), before slowly increasing as the ionized component comes in. The decrease continues the longest when $i = 80$ degrees. The open stars begin at $F_x/F_{\text{disc}} = 4.16$ when $\Gamma = 1.5$ and trace the ionized evolution. All four panels show the same decrease-increase behaviour with the absolute value decreasing with incidence angle. From these curves and the photon-index range of MCG–6–30–15 (1.8–2.1) we can conclude that the EW evolution of MCG–6–30–15 is consistent with that of a single purely neutral line, or of a hybrid line that is excited by radiation at a large incidence angle. However, this cannot explain the strange variation in line flux which may be indicative of more than one emission component. Indeed, both types of models can fit the data (Ballantyne & Fabian 2001).

4.3 Neutral and ionized Fe K α lines

The calculations presented here predict that ionized Fe K α lines at ~ 6.7 keV should be common in almost all cases if $F_x/F_{\text{disc}} \gg 1$. Evidence for ionized lines have been seen in the X-ray spectra

of some Narrow Line Seyfert 1 Galaxies (Comastri et al. 1998, 2001; Turner, George & Nandra 1998; Vaughan et al. 1999; Balantyne, Iwasawa & Fabian 2001; Turner et al. 2001a,b) and high-luminosity Seyferts/low-luminosity quasars (Reeves et al. 2000; Pounds et al. 2001; Orr et al. 2001), both of which are thought to be high accretion rate objects and so might not be directly applicable to the current computations. Most Seyfert galaxies seem to exhibit lines of neutral Fe at 6.4 keV (e.g. Nandra et al. 1997a), although this may be a result of contamination from a narrow component. Taking these results at face value suggests that discs are either weakly illuminated (i.e., $F_x/F_{\text{disc}} < 1$) or much denser than previously considered.

If discs are weakly illuminated then it is difficult to reconcile this with the otherwise very successful theory of coronal heating by magnetic flares which necessarily predicts a highly irradiated disc. It is possible that measurements of the centroid energy of the Fe K α line can be confused by poor signal-to-noise data, calibration problems, or gravitational redshifting effects. Searching for EW variations with the photon index through relations shown in Fig. 8 may provide an alternative test for determining the ionization state of the Fe K α line.

Extensions to the basic magnetic flare model can also reconcile the models with the data. For example, Nayakshin et al. (2000), Nayakshin (2000) and Done & Nayakshin (2001) discuss the idea that a local wind will be driven by a magnetic flare event. These authors argue that as a result of this wind, surface material on the disc will be blown away revealing denser gas deeper into the disc. It is this gas that produces the observed reflection spectrum complete with a neutral Fe K α line. However, the effects (or even the existence) of such an X-ray driven wind has not been properly modelled, so, in light of the results of this paper, the following model is proposed as an alternative.

Consider the situation when separate magnetic flares are occurring over the accretion disc (see Figure 10 and Merloni & Fabian 2001). Directly underneath each illuminating event, the surface of the disc is highly ionized and therefore produces no Fe K α emission. As the angle of incidence of the radiation increases, the flux incident on the gas drops resulting in ionized Fe K α lines. As the incidence angle further increases, the local F_x/F_{disc} decreases until eventually neutral lines dominate. Such a gradient in ionization on the disc has also been considered by Reynolds (2000) for AGN and by Done & Życki (1999), Young et al. (2001) and Done & Nayakshin (2001) to explain the low reflection fractions observed in low-state Galactic Black Hole Candidates. Since there is much more surface area on the disc that is weakly illuminated and/or illuminated at grazing incidence, the majority of the line emission detected by a telescope will be at neutral energies. This effect should work for any value of Γ , as the combination of low F_x/F_{disc} and large i will result in a neutral line (Fig. 4). Similarly, the complete ionization below each flare can occur at any photon-index, but its assurance will depend on the physical and geometrical details of the event itself.

Spectral evolution of the illumination events will also cause changes in the ionization state of the Fe K α line. The recent *RXTE* observation of the black hole candidate GX 339-4 reported by Feng et al. (2001) showed that as the X-ray flux decreased from its low state to an ‘‘off state’’, its Fe K α line evolved from neutral at 6.4 keV to ionized at 6.7 keV. More importantly, the photon index of the continuum evolved from about 1.5 to 2.2 as the flux decreased. As discussed earlier (Sect 4.1), when $\Gamma = 1.5$ the thermal ionization instability can operate and a neutral line is expected, but it is highly unlikely to work when $\Gamma = 2.2$, and a 6.7 keV line would be ob-

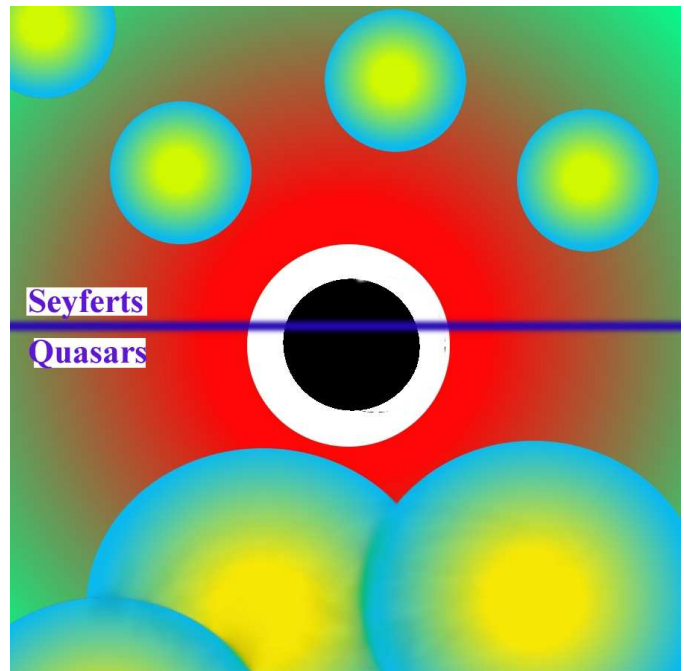


Figure 10. A schematic picture of how ionization gradients may effect observations of the Fe K α line. This illustration shows from a polar viewpoint an accretion disc (large red to green gradient) around a black hole. On top of the accretion disc magnetic flares are occurring (yellow-blue regions). In the top half of the figure the illumination events are fairly small and localized. Therefore, although they may highly ionize the gas directly below them (yellow regions), the amount of area that is producing strong ionized iron lines at 6.7 keV (blue regions) is relatively small compared to the area of the disc that is weakly illuminated. Therefore, a strong neutral line will be observed. This description might be appropriate for lower-luminosity objects such as Seyferts. The bottom half of the figure shows more powerful and (perhaps) more numerous magnetic flares. In this case, there are large areas of the disc that are completely ionized and so only a weak Fe K α line may be detected. This could explain the X-ray Baldwin effect in quasars if the higher luminosity in these objects translates into a more active corona.

served. Perhaps this is an observation of a decaying and expanding flare.

4.3.1 X-ray Baldwin effect

Observations of many Seyfert galaxies and quasars by *ASCA* have shown that as the X-ray luminosity of the source increases, the EW of the Fe K α line decreases until it becomes undetectable at a 2–10 keV luminosity of 10^{46} erg s $^{-1}$ (Iwasawa & Taniguchi 1993; Nandra et al. 1997b; Reeves & Turner 2000). This trend has been named the X-ray Baldwin effect in analogy to the decrease in EW of the C IV $\lambda 1550$ line in the UV continuum of QSOs (Baldwin 1977). In terms of the constant density models, this effect could easily be explained as the ionization parameter of the gas increasing to the point where the outer layers of the disc are fully ionized and therefore would not imprint any line emission on the reflection spectrum. The ionization parameter would increase if the higher luminosity in quasars was due to a higher accretion rate (Matt et al. 1993). Newer hydrostatic disc models also can explain the X-ray Baldwin effect by ionizing a thick skin on the surface of the accretion disk (Nayakshin 2000; Życki & Różańska 2001).

As discussed earlier, ionization gradients along the accretion disc by different flare locations may be able to account for the ob-

served energies of the Fe $K\alpha$ line. If the power and number of flares above the disk increases as one moves from Seyferts to quasars then this would increase the X-ray luminosity, and also increase the amount of surface area that is subject to a highly ionizing flux (see Fig. 10). In such a situation only a very weak, highly ionized Fe $K\alpha$ line would be emitted from the surface. Indeed, recent *XMM-Newton* observations show that ionized lines are observed in higher-luminosity objects (Reeves et al. 2001; Pounds et al. 2001).

Such a scenario is not too different from that envisaged by the other models, but suggests a more complex geometry. There are a number of details to work out in order for such a model to be placed on firm theoretical ground. Clearly, in a situation such as the one presented in the lower part of Fig. 10, feedback effects between the reflection spectrum and the coronal activity would be vitally important and may even assist in erasing spectral features through Comptonization (Petrucci et al. 2001).

5 CONCLUSIONS

The broad Fe $K\alpha$ line which (most likely) results from reflection from an accretion disc is the most important spectral signature in the X-ray study of AGN. The model calculations presented in this paper have shown that the behaviour and properties of the Fe line from an irradiated disc in equilibrium depend on how it is illuminated. Specifically, when the incident flux is larger than the disc flux, we predict that a He-like Fe $K\alpha$ line at 6.7 keV will be a common feature in the reflection spectrum. The thermal ionization instability is able to change this and produce a neutral line at 6.4 keV, but only when $\Gamma \leq 1.6$ (for a cutoff energy of 100 keV) and the incident flux is not too high.

The Fe $K\alpha$ EW will remain roughly constant as F_x/F_{disc} is increased until the atmosphere becomes highly ionized and then it will decrease to small values. The rate of decline is lower for higher values of Γ . When the line complex is dominated by He-like Fe, the EW will strongly increase with Γ , but will slightly decline with the photon-index if it is neutral. This effect could be used as an observational diagnostic to determine the ionization state of the line, independent of the line centroid.

Long observations of Seyferts & quasars by *XMM-Newton* would be required to test the predictions of the models. However, any narrow component to the line profile must be taken into account before a comparison could be made. The results of such a study would be important, as it is clear that the ionization state of the disc depends greatly on how it is irradiated which would greatly constrain coronal models.

The prediction that ionized lines are common can be reconciled with their observational rarity by employing multiple ionization gradients on the accretion disc, which would be a natural result of a magnetically active and patchy corona. The challenge is now extended to modellers to compute observationally testable predictions for such complex scenarios.

ACKNOWLEDGMENTS

The authors thank A. Fabian, S. Vaughan, K. Iwasawa & A. Merloni for valuable discussions, and C. Berger for assistance with the models. DRB acknowledges financial support from the Commonwealth Scholarship and Fellowship Plan and the Natural Sciences and Engineering Research Council of Canada. RRR acknowledges support from the College of the Holy Cross.

REFERENCES

- Baldwin J.A., 1977, *ApJ*, 214, 679
 Ballantyne D.R., Fabian A.C., 2001, *MNRAS*, 328, L11
 Ballantyne D.R., Iwasawa K., Fabian A.C., 2001, *MNRAS*, 323, 506
 Ballantyne D.R., Ross R.R., Fabian A.C., 2001, *MNRAS*, 327, 10
 Ballantyne D.R., Ross R.R., Fabian A.C., 2002, in Ferland G.J., Savin D.W., eds., *Spectroscopic Challenges of Photoionized Plasmas*, ASP Conference Series, in press (astro-ph/0102268)
 Beloborodov A.M., 1999, *ApJ*, 510, L123
 Chiang J., Reynolds C.S., Blaes O.M., Nowak M.A., Murray N., Madejski G., Marshall H.L., Magdziarz P., 2000, *ApJ*, 528, 292
 Comastri A., et al., 1998, *A&A*, 333, 31
 Comastri A., et al., 2001, *A&A*, 365, 400
 Done C., Życki P., 1999, *MNRAS*, 305, 457
 Done C., Nayakshin S., 2001, *MNRAS*, 328, 616
 Fabian A.C., Rees M.J., Stella L., White N.E., 1989, *MNRAS*, 238, 729
 Fabian A.C., Nandra K., Reynolds C.S., Brandt W.N., Otani C., Tanaka Y., Inoue H., Iwasawa K., 1995, *MNRAS*, 277, L11
 Fabian A.C., Iwasawa K., Reynolds C.S., Young A.J., 2000, *PASP*, 112, 1145
 Feng Y.X., Zhang S.N., Sun X., Durouchoux Ph., Chen W., Cui W., 2001, *ApJ*, 553, 394
 Galeev A.A., Rosner R. & Vaiana G.S., 1979, *ApJ*, 229, 318
 Gebhardt K., et al., 2000, *ApJ*, 539, L13
 George I.M., Fabian A.C., 1991, *MNRAS*, 249, 352
 George I.M., Turner T.J., Yaqoob T., Netzer H., Laor A., Mushotzky R.F., Nandra K., Takahashi T., 2000, *ApJ*, 531, 52
 Guilbert P.W., Fabian A.C., McCray R., 1983, *ApJ*, 266, 466
 Guilbert P.W., Rees M.J., 1988, *MNRAS*, 233, 475
 Haardt F., Maraschi L., 1991, *ApJ*, 380, L51
 Haardt F., Maraschi L., Ghisellini G., 1994, *ApJ*, 432, L95
 Iwasawa K., Taniguchi Y., 1993, *ApJ*, 413, L15
 Iwasawa K., et al., 1996, *MNRAS*, 282, 1038
 Iwasawa K., Fabian A.C., Young A.J., Inoue H., Matsumoto C., 1999, *MNRAS*, 306, L19
 Kaspi S., et al., 2001, *ApJ*, 554, 216
 Krolik J.H., McKee C.F., Tarter, C.B., 1981, *ApJ*, 249, 422
 Krolik J.H., Madau P., Życki P.T., 1994, *ApJ*, 420, L57
 Lee J.C., Fabian A.C., Reynolds C.S., Brandt W.N., Iwasawa K., 2000, *MNRAS*, 318, 857
 Li Y., Gu M.F., Kahn S.M., 2001, *ApJ*, submitted (astro-ph/0106163)
 Lightman A.P., White T.R., 1988, *ApJ*, 335, 57
 Lubiński P., Zdziarski A.A., 2001, *MNRAS*, 323, L37
 Magdziarz P., Zdziarski A.A., 1995, *MNRAS*, 273, 837
 Malzac J., Beloborodov A.M., Poutanen J., 2001, *MNRAS*, 326, 417
 Matt G., 2000, in *Proc. X-Ray Astronomy '99* (September 6-10, Bologna, Italy), in press (astro-ph/0007105)
 Matt G., Perola G.C., Piro L., 1991, *A&A*, 247, 27
 Matt G., Fabian A.C., Ross R.R., 1993, *MNRAS*, 262, 179
 Matt G., Fabian A.C., Ross R.R., 1996, *MNRAS*, 278, 1111
 Merloni A., Fabian A.C., 2001, *MNRAS*, 328, 958
 Merloni A., Fabian A.C., Ross R.R., 2000, *MNRAS*, 313, 193
 Morales R., Fabian A.C., 2002, *MNRAS*, 329, 209
 Morrison R., McCammon D., 1983, *ApJ*, 270, 119
 Mushotzky R.F., Done C., Pounds K.A., 1993, *ARA&A*, 31, 717
 Nandra K., George I.M., Mushotzky R.F., Turner T.J., Yaqoob T., 1997a, *ApJ*, 477, 602

Nandra K., George I.M., Mushotzky R.F., Turner T.J., Yaqoob T., 1997b, *ApJ*, 488, L91

Nandra K., George I.M., Mushotzky R.F., Turner T.J., Yaqoob T., 1999, *ApJ*, 523, L17

Nayakshin S., 2000, *ApJ*, 540, L37

Nayakshin S., Kallman T., 2001, *ApJ*, 546, 406

Nayakshin S., Kazanas D., 2002, *ApJ*, in press (astro-ph/0106450)

Nayakshin S., Kazanas D., Kallman T., 2000, *ApJ*, 537, 833

Oelgoetz J., Pradhan A.K., 2001, *MNRAS*, 327, L42

Orr A., Barr P., Guainazzi M., Parmar A.N., Young A.J., 2001, *A&A*, 376, 413

Péquignot D. et al., 2002, in Ferland G.J., Savin D.W., eds., *Spectroscopic Challenges of Photoionized Plasmas*, ASP Conference Series, in press

Petrucchi P.-O., Merloni A., Fabian A.C., Haardt F., Gallo E., 2001, *MNRAS*, 328, 501

Pounds K., Reeves J., O'Brien P., Page K., Turner M., Nayakshin S., 2001, *ApJ*, 559, 181

Poutanen J., Fabian A.C., 1999, *MNRAS*, 306, L31

Reeves J.N., Turner M.J.L., 2000, *MNRAS*, 316, 234

Reeves J.N., et al., 2000, *MNRAS*, 312, L17

Reeves J.N., et al., 2001, *A&A*, 365, L134

Reynolds C.S., 1997, *MNRAS*, 286, 513

Reynolds C.S., 2000, *ApJ*, 533, 811

Reynolds C.S., 2001, in Peterson B.A., Polidan R.S., Pogge R.W., eds., *Probing the Physics of Active Galactic Nuclei by Multi-wavelength Monitoring*, ASP Conference Series Vol. 224, 105

Reynolds C.S., Wilms J., 2000, *ApJ*, 533, 821

Ross R.R., 1978, PhD thesis, University of Colorado

Ross R.R., Fabian A.C., 1993, *MNRAS*, 261, 74

Ross R.R., Weaver R., McCray R., 1978, *ApJ*, 219, 292

Ross R.R., Fabian A.C., Brandt W.N., 1996, *MNRAS*, 278, 1082

Ross R.R., Fabian A.C., Young A.J., 1999, *MNRAS*, 306, 461

Rózańska A., 1999, *MNRAS*, 308, 751

Rózańska A., Dumont A.-M., Czerny B., Collin S., 2001, in Yaqoob T., Krolik J.H., eds., *the proceedings of X-ray Emission from Accretion onto Black Holes*, published electronically (<http://www.pha.jhu.edu/groups/astro/workshop2001/>)

Ruszkowski M., 2000, *MNRAS*, 315, 1

Rybicki G.B., Lightman A.P., 1979, *Radiative Processes in Astrophysics*, Wiley

Shakura N.I., Sunyaev R.A., 1973, *A&A*, 24, 337

Svensson R., 1996, *A&AS*, 120, 475

Svensson R., Zdziarski A.A., 1994, *ApJ*, 436, 599

Tanaka T., et al., 1995, *Nature*, 375, 659

Turner T.J., George I.M., Nandra K., 1998, *ApJ*, 508, 648

Turner T.J., et al., 2001a, *ApJ*, 548, L13

Turner T.J., et al., 2001b, *ApJ*, 561, 131

Vaughan S., Edelson R., 2001, *ApJ*, 548, 694

Vaughan S., Pounds K.A., Reeves J., Warwick R., Edelson R., 1999, *MNRAS*, 308, L34

Wang J.X., Zhou Y.Y., Xu H.G., Wang T.G., 1999, *ApJ*, 516, L65

Wang J.X., Wang T.G., Zhou Y.Y., 2001, *ApJ*, 549, 891

Weaver K.A., Gelbord J., Yaqoob T., 2001, *ApJ*, 550, 261

Yaqoob T., George I.M., Nandra K., Turner T.J., Serlemitsos P.J., Mushotzky R.F., 2001, *ApJ*, 546, 759

Yaqoob T., Padmanabhan U., Dotani T., Nandra K., 2002, *ApJ*, in press (astro-ph/0112318)

Young A.J., Fabian A.C., Ross R.R., Tanaka Y., 2001, *MNRAS*, 325, 1045

Życki P.T., Krolik J.H., Zdziarski A.A., Kallman T.R., 1994, *ApJ*, 437, 597

Życki P.T., Rózańska A., 2001, *MNRAS*, 325, 197

This paper has been typeset from a $\text{\TeX}/\text{\LaTeX}$ file prepared by the author.